

斜め伝搬ホイッスラーモード波動粒子相互作用のテスト粒子シミュレーション

Test Particle Simulation on Wave-Particle Interactions of Obliquely Propagating Whistler-mode Waves

研究代表者 : 謝 怡凱 (京大生存圏研究所)
yikai_hsieh@rish.kyoto-u.ac.jp

研究分担者 : 大村 善治 (京大生存圏研究所)
omura@rish.kyoto-u.ac.jp
担当 : 計算結果の理論的検討

長尾 龍一 (京大生存圏研究所)
nagao.ryuichi.77m@st.kyoto-u.ac.jp
担当 : Upper-band コーラスと電子の三次元計算機実験の計算

研究目的 (Research Objective):

The energetic electron precipitation (EEP) induced by chorus waves is the main cause of pulsating auroras and one of the processes removing energetic electrons from the Earth's outer radiation belt. Several simulations provided direct evidence showing the chorus-driven EEP (i. e., Rosenberg et al. (1990), Hikishima et al. (2010), and Miyoshi et al. (2010)). However, the simulations are all under the parallel propagation assumption. Oblique whistler mode wave-particle interactions accelerate electrons and lower their equatorial pitch angles via Landau resonance efficiently. Landau resonance does not occur in parallel wave-particle interactions. Based on this phenomenon, the Landau resonance should contribute to the precipitation of 10–100 keV electrons or even relativistic electrons. From in situ observations, there are many events of oblique chorus emissions in the Earth's magnetic field. The relation between chorus-driven EEP and the Landau resonance has not been clarified yet. In this study we check the process of oblique chorus induced EEP and how important the wave normal angles contribute to the precipitation by test-particle simulations.

計算手法 (Computational Aspects):

Test-particle simulations and Green's function method are applied to calculate the wave-particle interactions between chorus emissions and energetic electrons. Our target location is around an L=4.5 shell in the Earth's magnetosphere. About the wave models, generally, we have a pair of emissions propagate from the equator toward high latitudes. Subpacket structures are applied for wave amplitudes, and rising tone is employed for wave frequencies. We have 4 Green's function sets. For cases 1–3, the maximum amplitudes are 2.1 nT and the maximum wave normal angles are 0°, 20°, and 60°, respectively. For case 4, the maximum amplitude is 370 pT and the maximum wave normal angle is 60°. Fig 1 shows the

wave model of case 4. A Green's function $G(K, K_0, \alpha, \alpha_0, \Phi, \Phi_0)$ is a result in (K, α, Φ) of a group of electrons initially at (K_0, α_0, Φ_0) , where K , α , and Φ are kinetic energy, equatorial pitch angle, and longitude, respectively, interacting with a pair of emission. For one Green's function, we input 3600 electrons in test particle simulation. For a Green's function set, we calculate K_0 from 10 keV to 6 MeV and α_0 from 5° to 89° . We submitted 183,600,000 electrons for one set. Both MPI and OpenMP methods are employed for parallel computing. After generating the Green's functions, we applied the convolution integral method to simulate electrons interacting with consecutive emissions.

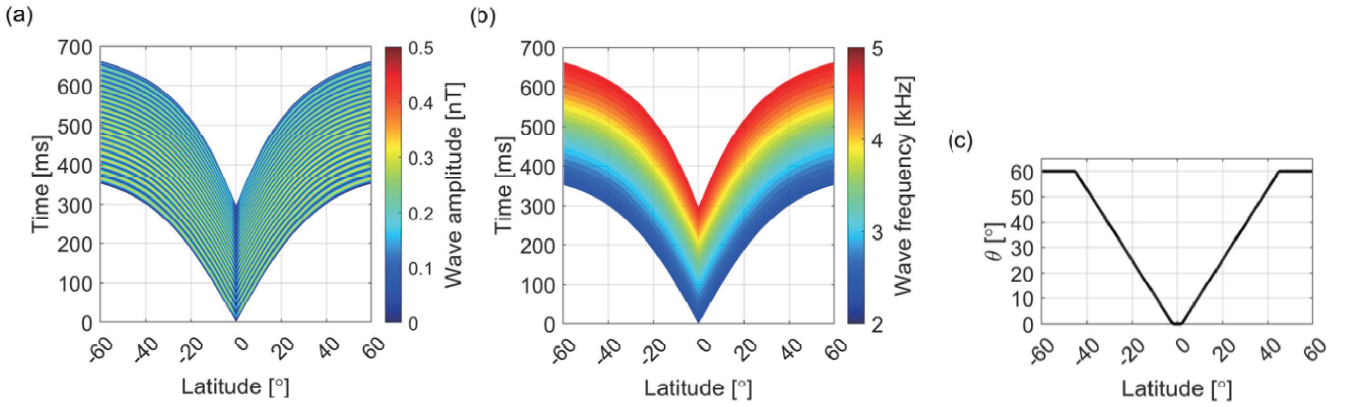


Fig.1 Wave model of Case 4 for test particle simulation.

研究成果 (Accomplishments) :

We focused on the results of electrons precipitating from the magnetosphere into the atmosphere, namely, the electrons with $\alpha < \text{loss cone angle } 4.56^\circ$. We verified the contributions of different wave normal angles and wave amplitudes to electron precipitation.

1. Pitch Angle Scatterings among different wave normal angles

We test electrons initially at high equatorial pitch angles for cases 1–3 to test the pitch angle scattering rates among different wave normal angles. The wave amplitude is a control variable in this comparison. We found that low-equatorial-pitch-angle electrons can be moved to the loss cone within 3 emissions. While it requires more interaction cycles, namely longer interaction time, for high-equatorial-pitch-angle electrons to approach the loss cone. Fig 2 shows the electron distributions after interaction cycles 1, 5, and 10, for MeV electrons. Fig 2 indicates that a larger wave normal angle contributes to a higher pitch angle scattering rate. Fig 3a is electron precipitation fluxes after 2 mins and 5 mins from the beginning of chorus events. The figure clearly shows that a higher wave normal angle causes larger electron precipitation. The reason is Landau resonance. Nonlinear trapping via Landau resonance can low equatorial pitch angle of resonant electrons. A larger wave normal angle contributes to stronger Landau resonance and causes stronger electron precipitation.

2. Comparison precipitation fluxes between different wave amplitudes

Fig 3b and 3c are precipitation fluxes of case 3 and case 4, respectively. The wave normal angle is the control variable here. Obviously, the figures tell that amplitude highly affects precipitation. A larger wave amplitude case has more electron precipitation fluxes in all energies.

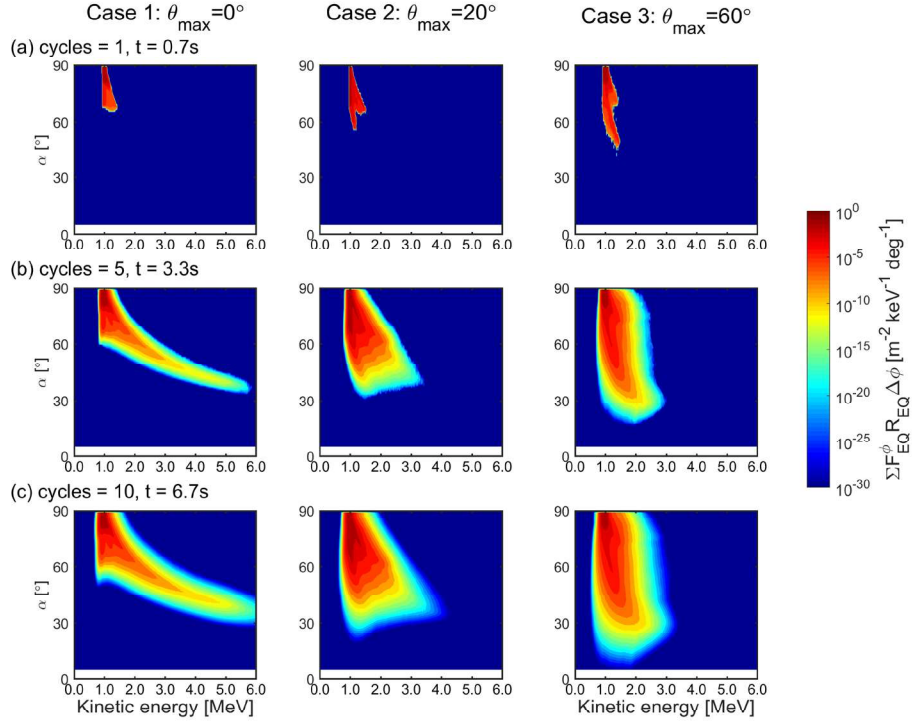


Fig.2 Comparison of pitch angle scattering rate among different wave normal angles.

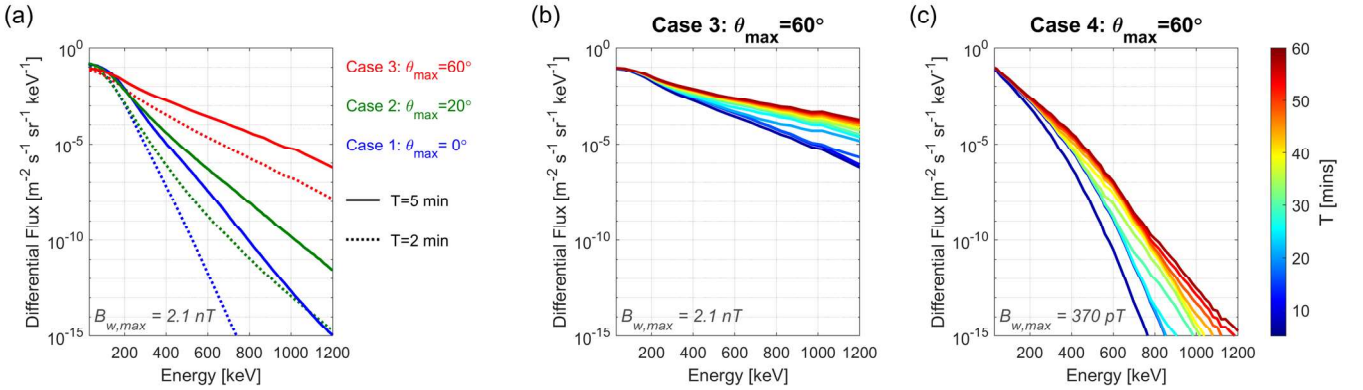


Fig.3 Precipitated electron fluxes for different wave normal angles and wave amplitudes.

3. Two-Step Precipitation Process in Oblique Wave-Particle Interaction

Previously (The KDK 2020 report) we have verified that Landau resonance is not able to scatter the electron into the loss cone. Most of the precipitation is directly caused by cyclotron resonance. Based on this description and the results shown above, we propose a two-step precipitation process for oblique chorus emissions that contributes to more electron loss:

(a) Through Landau resonance interaction with a chorus emission, electrons at high pitch angles are effectively accelerated in the parallel direction, and their pitch angles become

lower.

(b) The electrons bounce back toward the equator, and they are pushed into the loss cone through nonlinear scattering due to cyclotron resonance with another chorus emission. The combination of Landau resonance and cyclotron resonance by oblique chorus emissions results in a higher precipitation rate than the single cyclotron resonance by purely parallel chorus emissions.

公表状況 (Publications) :

(論文)

1. Hsieh, Y.-K., Omura, Y., & Kubota, Y. (2022). Energetic electron precipitation induced by oblique whistler mode chorus emissions. *Journal of Geophysical Research: Space Physics*, 127, e2021JA029583. <https://doi.org/10.1029/2021JA029583>

(口頭)

1. Hsieh, Y.-K., Y. Omura, Simulation on energetic electron precipitation induced by whistler mode chorus emissions in the outer radiation belt, American Geophysical Union (AGU) 2021 Fall Meeting, New Orleans & Online, Dec 2021.
2. 謝怡凱, 大村善治, Role of nonlinear wave-particle interactions in energetic electron precipitation by oblique chorus emissions in the outer radiation belt, 地球電磁気・地球惑星圏学会 2021 年秋学会, オンライン, 2021 年 11 月.
3. Hsieh, Y.-K., Y. Omura, Modeling of energetic electron precipitation affected by oblique whistler mode chorus emissions in the outer radiation belt, The XXXIV General Assembly and Scientific Symposium (GASS) of the International Union of Radio Science (URSI), Online, Aug-Sep 2021.
4. Hsieh, Y.-K., Y. Omura, Precipitation process of electrons in the outer radiation belt associated with oblique whistler mode chorus emissions, Joint Scientific Assembly IAGA-IASPEI 2021, Online, Aug 2021.
5. Hsieh, Y.-K., Y. Omura, Energetic electron fluxes and precipitation at outer radiation belt associated with localized oblique whistler mode chorus emissions, Asia Oceania Geosciences Society (AOGS) 18th Annual Meeting, Online, Aug 2021. (Invited)
6. Hsieh, Y.-K., Y. Omura, Modeling of outer radiation belt electron dynamics associated with whistler mode chorus emissions via Green's function method, Japan Geoscience Union (JpGU) Meeting 2021, Online, May-June 2021.
7. Hsieh, Y.-K., Y. Omura, Energetic electron precipitation via oblique whistler mode chorus emissions in the outer radiation belt, EGU General Assembly 2021, Online, Apr 2021.